Catalysis Today 151 (2010) 237–243

Contents lists available at ScienceDirect

Catalysis Today

journal homepage: www.elsevier.com/locate/cattod

Heat of adsorption for NH_3, NO_2 and NO on Cu-Beta zeolite using microcalorimeter for NH_3 SCR applications

Norman Wilken [a], Krishna Kamasamudram [b], Neal W. Currier [b], Junhui Li [b], Aleksey Yezerets [b], Louise Olsson [a,*]

[a] Competence Centre for Catalysis, Chemical Reaction Engineering, Chalmers University of Technology, SE-412 96 Gothenburg, Sweden
[b] Cummins Inc., 1900 McKinley Ave., MC 50183, Columbus, IN 47201, USA

ARTICLE INFO

Article history:
Available online 19 March 2010

Keywords:
Calorimeter
DSC
NH_3
Cu-Beta
Zeolite
Heat of adsorption

ABSTRACT

Microcalorimetry is a powerful technique with which to measure the heat of adsorption (ΔH), producing values that are very important when developing kinetic models. The method provides a way of determining these parameters independently. For kinetic models describing NH_3 SCR it is critical to be able to accurately describe the storage of ammonia and NO_x in order to simulate rapid transients occurring in the experiments. The objective of our study is to measure the heat of adsorption of NH_3, NO_2 and NO on Cu-Beta. An ammonia TPD experiment was conducted at 150 °C using the microcalorimeter, resulting in the observation of an exotherm when introducing ammonia due to adsorption. This resulted in an average heat of adsorption of −100 kJ/mol. A good reproducibility was found when using a second sample, resulting in −97 kJ/mol. In order to investigate the coverage dependence of the heat of adsorption, an ammonia stepwise experiment was conducted. First, the catalyst was exposed to NH_3 at 500 °C, resulting in the adsorption of strongly bound ammonia and obtaining a heat of adsorption of −110 kJ/mol. Thereafter, the catalyst was cooled in Ar and at 400 °C, NH_3 was again introduced. Due to that the temperature is lower the ammonia that adsorbed was weaker. The procedure was repeated at 300, 200 and 100 °C, resulting in a coverage dependent activation energy for ammonia desorption (if assuming zero activation for adsorption) according to the following formula:

$$E_{desorption,\mathrm{NH_3}} = 120.0(1 - 0.38\theta_{\mathrm{NH_3}})$$

where $\theta_{\mathrm{NH_3}}$ is the coverage of ammonia on the surface. The NO and NO_2 adsorption and desorption were investigated using NO and NO_2 TPD experiments, respectively. For the NO_2 TPD experiment, approximately three NO_2 were stored for each NO produced, corresponding to the disproportionation mechanism. This resulted in ΔH of −65 kJ/mol per NO_2 consumed. The NO TPD experiment resulted in that only small amounts of NO was adsorbed.

1. Introduction

Diesel engine exhausts contain excess oxygen and a standard 3-way catalyst cannot reduce NO_x efficiently, due to oxygen poisoning of the noble metal sites. There are three major techniques for reducing NO_x in oxygen excess: (i) NO_x storage [1,2], (ii) hydrocarbon selective catalytic reduction (HC SCR) [3,4] and (iii) urea/ammonia (NH_3) SCR [5–10]. The focus of this study is on NH_3 SCR. The urea decomposes and hydrolyzes to form ammonia [11,12] according to the following reactions:

$$NH_2{-}CO{-}NH_2 \rightarrow NH_3 + HNCO \tag{1}$$

$$HNCO + H_2O \rightarrow NH_3 + CO_2 \tag{2}$$

The ammonia reacts selectively with NO_x to form N_2 and H_2O on a catalyst. The reaction rate depends on the source of the NO_x. The "standard SCR" reaction (see Eq. (3)) occurs with NO, rapid SCR (Eq. (4)) with 50% NO and 50% NO_2 and, finally, the slow NO_2 SCR step (Eq. (5)).

$$4NH_3 + 4NO + O_2 \rightarrow 4N_2 + 6H_2O \tag{3}$$

$$2NH_3 + NO + NO_2 \rightarrow 2N_2 + 3H_2O \tag{4}$$

$$4NH_3 + 3NO_2 \rightarrow 3.5N_2 + 6H_2O \tag{5}$$

There are several catalysts used for this system; important groups of catalysts include vanadia on titania [5,6,13,14], copper exchanged zeolites [8,15–19] and iron exchanged zeolites [7,19–24].

There are some kinetic models available for ammonia SCR on vanadia on titania [5,25–28], Cu-ZSM-5 [29–32], Cu-faujasite [33],

* Corresponding author. Fax: +46 031 772 4390.
E-mail address: louise.olsson@chalmers.se (L. Olsson).

0920-5861/$ – see front matter © 2010 Elsevier B.V. All rights reserved.
doi:10.1016/j.cattod.2010.02.002

H-ZSM-5 [34] and Fe zeolites [35–37]. In order to develop a kinetic model for ammonia SCR capable of describing transient effects, it is vital to have a good model for the ammonia and NO_x storage and release. Calorimetry is a powerful technique [38,39] for determining the heat of adsorption using independent experiments. Calorimetry has been used to determine the energetics associated with urea decomposition [11,12,40]. Furthermore, calorimetry has been used for determining the acid strength of acid zeolites with the use of ammonia adsorption. Felix et al. [41] obtained an average ΔH for ammonia of about −114 kJ/mol for H-ZSM-5 (SiO_2/Al_2O_3 ratio of 110). The heat of adsorption of ammonia for zero coverage was observed to be −130 kJ/mol for H-ZSM-5 (SiO_2/Al_2O_3 ratio of 30) [42], −130 kJ/mol for H-Beta (SiO_2/Al_2O_3 ratio of 19.6) [42] and −120 to 130 kJ/mol for H-ZSM-5 (SiO_2/Al_2O_3 ratio of 110) [41]. Further, Boskovic et al. [43] obtained an average ΔH of −104.8 kJ/mol for Cu-ZSM-5 (SiO_2/Al_2O_3 ratio of 30).

However, there are today no calorimetric measurements of the heat of adsorption for ammonia, NO_2 and NO on Cu-Beta zeolites. The objective of this work is to determine the heat of adsorption for these compounds on Cu-Beta and also investigate the coverage dependent ΔH for ammonia and the formation of nitrates. Diesel engine exhausts are rapidly varying in composition and temperature and it is, therefore, crucial to have a good description of the heat of adsorption in kinetic models for ammonia SCR.

2. Experimental

2.1. Catalyst preparation

The catalyst powder was prepared by aqueous ion-exchange (IE) of a beta zeolite with a silica to alumina ratio of 38, produced by Zeolyst International. To introduce controlled amount of copper, the powder zeolite was ion-exchanged in two stages, first with $NaNO_3$, followed by $Cu(CH_3COO)_2$. Fifty grams of zeolite was used and the details about the ion-exchange are presented in Table 1. Before making the copper ion-exchange, the zeolite was filtered and dried at 120 °C for 12 h. After the final copper exchange had been made, the zeolite was washed and dried. The powder was used in the calorimetric measurements. A monolith (21 mm in diameter and 20 mm long) was prepared. First a thin layer of alumina was added in order to facilitate the attachment of the zeolite. Boemithe (20 wt%) was used as a binder. Thereafter, the zeolite was applied using the incipient wetness technique. The weight of the alumina layer was 222 mg and the corresponding zeolite layer was 523 mg. The cell density was 400 cpsi.

2.2. Catalyst characterization

The particle size and shape of the H-Beta-38 powder was examined using a JEOL scanning electron microscope (SEM) of the JXA-8600 model. The copper content was measured using inductively coupled plasma and atomic emission spectrometry (ICP–AES).

2.3. Microcalorimeter measurements

Briefly, the experimental setup consisted of a gas mixing system, a calorimeter and an FTIR. The gas mixing system contained several mass flow controllers (MFC) and was used to produce the desired gas composition. The calorimeter (Setaram Sensys DSC) consisted of two quartz tubes. In one of them, the sample was placed on a sintered quartz bed, with the other tube serving as a reference. The FTIR (MultiGas^{TM} 2030 HS) was used to analyze the composition of the gases after the calorimeter. The total flow through the sample was 100 ml/min, with Ar as inert balance. In order to increase the time resolution in the FTIR, the gas out from the calorimeter was diluted with 400 ml/min Ar. A sample of approximately 100 mg was used in the measurements. Two powder samples were used, both from the same batch, and denoted as "Powder I" and "Powder II" weighing 99.9 and 100.3 mg, respectively. Prior to use, both powders were aged for 2 h in the calorimeter at 650 °C using a total flow of 200 ml/min, and the gas composition of 8% O_2, 400 ppm NO and 400 ppm NH_3. An NH_3 temperature programmed desorption (TPD) experiment was conducted on both samples in order to ensure reproducible results. The NO_2 TPD was done on Powder I, whereas the NH_3 stepwise experiment and NO TPD were applied on Powder II. The experimental details are provided below.

Prior to all experiments, the catalyst was pretreated for 15 min with 8% O_2 at 500 °C. For the TPD experiments, the temperature was decreased to 150 °C after the pretreatment. Following this, the catalyst was exposed for 60 min to 2000 ppm NH_3 (or NO or NO_2), followed by an exposure for 50 min to Ar alone. Thereafter, the temperature was increased at a rate of 40 °C/min to 600 °C.

In order to get information about the coverage dependent heat of adsorption for ammonia, an ammonia stepwise experiment was conducted. After the pretreatment, the catalyst was exposed to 2000 ppm NH_3 at 500 °C over a period of 60 min. Because the loosely bound ammonia would not adsorb at such a high temperature, this procedure resulted in the adsorption of the strongly bound ammonia. Following this, the catalyst was exposed to Ar alone for 50 min, and then lowering the temperature to 400 °C. The same procedure was repeated at 400 °C (60 min of 2000 ppm NH_3 followed by 50 min Ar alone). These steps were conducted at 300 °C, 200 °C and, finally, at 100 °C. When the temperature was lowered, the more loosely bound ammonia was adsorbed. In this way, it was possible to gain knowledge of the coverage dependent heat of adsorption.

2.4. Flow reactor experiment

Briefly, the flow reactor consisted of a quartz tube into which the catalyst was placed. A thermo couple was placed about 10 mm in front of the catalyst to control the temperature. A second thermocouple was placed inside the catalyst. The gases were then mixed by using several mass flow controllers and one liquid controller. The gases after the reactor were analyzed using an FTIR (MultiGas^{TM} 2030 HS).

Prior to use, the monolith was aged at 650 °C, with 8% O_2, 400 ppm NO, 400 ppm NH_3, 6% H_2O and 5% CO_2. The steady state NO SCR activity was examined at 150, 200, 250, 300, 350, 400 and 500 °C, using 8% O_2, 400 ppm NO, 400 ppm NH_3, 6% H_2O and 5% CO_2. The total flow was 3500 ml/min, resulting in a space velocity of 30 300 h^{-1}.

Table 1
Description of the ion-exchange with sodium and copper.

Sequence of exchange	Water volume (ml)	Mass $NaNO_3/(CH_3COO)_2Cu$ (g)	Ion-exchange time (h)	pH value
1.	500	4.59 ($NaNO_3$)	1.0	6.6
2.	500	4.60 ($NaNO_3$)	0.17	6.3
3.	1500	3.0 $(CH_3COO)_2Cu$	12	~6
4.	1500	3.2 $(CH_3COO)_2Cu$	12	~6
5.	1500	3.4 $(CH_3COO)_2Cu$	12	~6

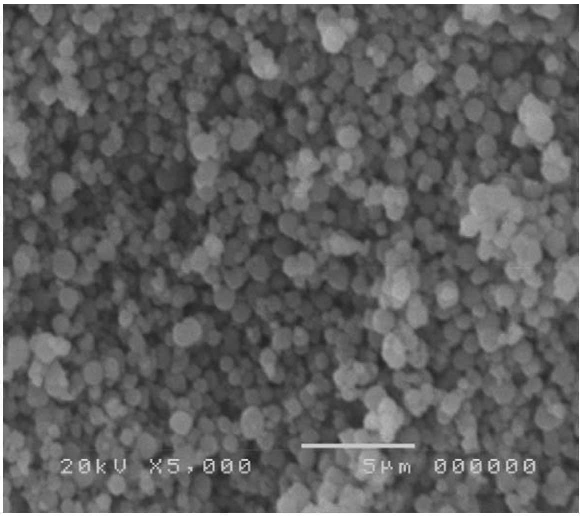

Fig. 1. SEM picture of the H-Beta powder from Zeolyst International. The length scale shown in the picture is 5 μm.

3. Results and discussion

3.1. Catalyst characterization

If the zeolite crystals are large it can cause mass-transport limitations. This will affect the activity and selectivity of the catalyst. In order to investigate the particle sizes we used SEM measurements. In Fig. 1, the resulting SEM picture from the H-Beta powder is shown. It can be observed that the particles are spherical and small, about 1 μm. Since the particles are very small it reduces the risk of having internal mass-transport limitations within the particles.

The copper amount was determined using inductively coupled plasma and atomic emission spectrometry (ICP–AES), resulting in 4.0 wt%.

3.2. Flow reactor measurements

The NO SCR activity was investigated with the monolith sample using a flow reactor. The purpose of this measurement was to ensure that the prepared catalyst showed a good SCR activity. The catalyst was first aged at 650 °C. Thereafter, an activity measurement was conducted using a gas composition of 8% O_2, 400 ppm NO, 400 ppm NH_3, 6% H_2O and 5% CO_2. The measured NH_3, NO and NO_2 concentrations are shown in Fig. 2. At 150 °C, a small conversion of 10% was observed, but when the temperature increased to 200 °C, a conversion of more than 80% was obtained. There is an equimolar consumption of NO and NH_3, which has been previously observed for standard SCR over copper zeolites [8]. At higher temperatures, the conversion of NH_3 was 100% because a combination of standard SCR and the ammonia oxidation. The oxidation of ammonia also caused a decrease in the conversion of NO_x at higher temperatures. In addition, small amounts of N_2O are observed. At all temperatures the NO_2 production was low.

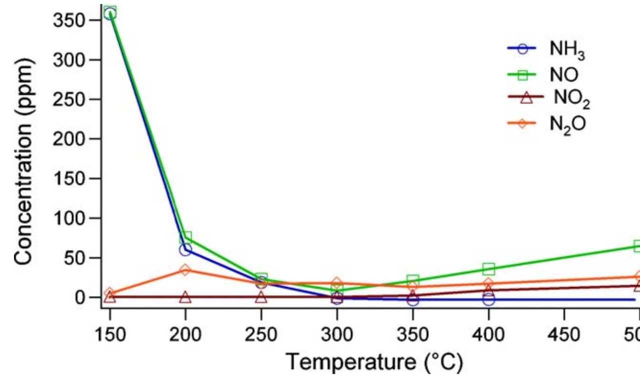

Fig. 2. Steady state concentrations of NH_3, NO and NO_2. The inlet gas concentration was 8% O_2, 400 ppm NO, 400 ppm NH_3, 6% H_2O and 5% CO_2.

3.3. Microcalorimeter measurements

An ammonia TPD experiment was conducted using the microcalorimeter in combination with FTIR in order to measure the heat of adsorption of ammonia. The results of the thermogram and FTIR are shown in Fig. 3. The catalyst was first oxidized by using 8% O_2 at 500 °C in order to ensure the removal of all ammonia from the surface. The temperature was than lowered to 150 °C and

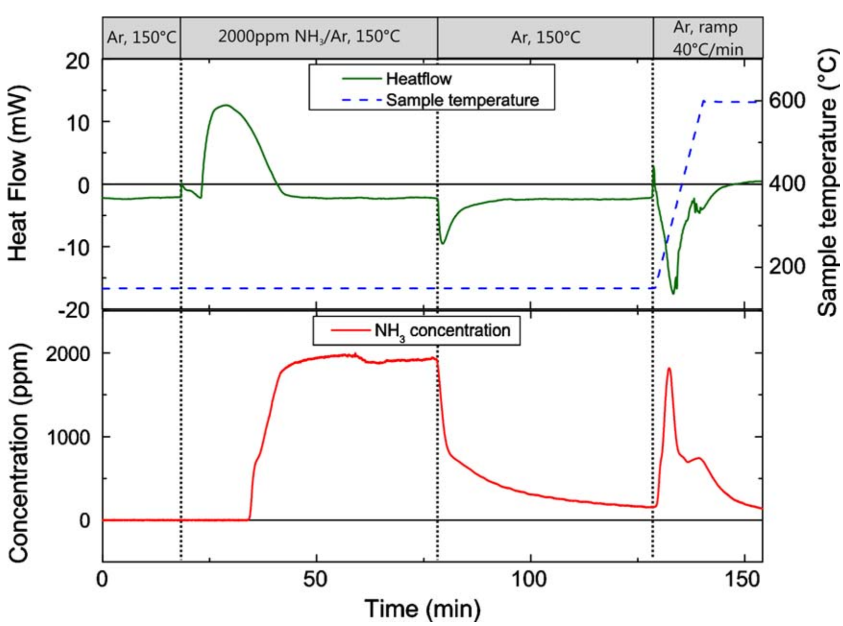

Fig. 3. Thermogram and FTIR signal for an NH_3 TPD experiment on a Cu-Beta catalyst.

after about 20 min, 2000 ppm ammonia was introduced. A large exotherm was observed; no NH_3 was simultaneously observed in the gas outlet. This means that all ammonia was adsorbed on the catalyst. Further, the catalyst was placed on a sintered plate, with the flow behaving like a plug flow reactor [44]. Ammonia has a high sticking probability, likely resulting in that the coverage of ammonia was first high in the inlet of the bed and close to zero in the outlet. This ammonia front then moved down the bed and after about 35 min, the ammonia broke through. Consequently, we were observing an average heat of adsorption as the coverage front moved down the bed. In other experiments (not shown here) with lower flows, the heat signal was constant for several min during the adsorption. In this experiment (see Fig. 3), the heat signal was about 14.8 mW during adsorption and all ammonia (2000 ppm) was simultaneously consumed, corresponding to an average heat of adsorption of −100 kJ/mol. This was similar to −104.8 kJ/mol, the heat of adsorption of ammonia that Boskovic et al. [43] obtained on Cu-ZSM-5 (SiO_2/Al_2O_3 ratio of 30) after exposing it to ammonia for 1 h. Felix et al. [41] obtained an average ΔH of about −114 kJ/mol for H-ZSM-5 (SiO_2/Al_2O_3 ratio of 110). Thus, there seems to be large similarities in the adsorption strength between the samples.

After the ammonia adsorption phase, the catalyst was exposed to Ar alone; an endotherm was observed due to desorption of loosely bound ammonia. Also, ammonia desorption was visible in the gas outlet. After 50 min, the temperature ramp (40 °C/min) was started and a desorption peak was observed with a corresponding endotherm. This experiment was conducted with Powder I (see Section 2). A sample from the same batch of Cu-Beta was used; this sample was denoted Powder II. The ammonia TPD was repeated for this sample, resulting in 14.4 mW and a corresponding heat of adsorption of −97 kJ/mol. Thus the samples and experiments showed good reproducibility.

For H-ZSM-5 calorimetric results have demonstrated a coverage dependent heat of adsorption for ammonia [41]. Further, in several kinetic models it was necessary to include a coverage dependent activation energy for desorption [29,32,41,45–47] according to the following equation:

$$E_{desorption,j} = E_{desorption,j}(0)(1 - \alpha_{i,j}\theta_i) \quad (6)$$

where θ_i is the coverage of compound i; $\alpha_{i,j}$ is a constant describing coverage dependent activation energy for compound i in reaction j.

This form of the activation energy is important to describe the broad nature of the ammonia desorption peak. For a kinetic model, it is vital to have a good description of the ammonia adsorption and desorption processes in order to adequately account for transients [29]. To gain more information about the coverage dependent activation energy, we conducted an ammonia stepwise experiment. Briefly, the catalyst was exposed to 2000 ppm NH_3 at a high temperature (500 °C), which caused adsorption of strongly bound ammonia. The loosely bound ammonia would not be adsorbed at such a high temperature. Thereafter, the catalyst was flushed with Ar and then cooled to 400 °C. At this point, all the sites with high adsorption energy were already occupied and when the catalyst was again exposed to 2000 ppm ammonia, the weaker sites were occupied. These steps were repeated at 300, 200 and 100 °C. The resulting thermogram and FTIR signal are shown in Fig. 4. At 500 °C, an exotherm of 16.3 mW was observed and all ammonia was simultaneously adsorbed. This caused a heat of adsorption of −110 kJ/mol. After about 6 min, the ammonia broke through and reached the inlet value of 2000 ppm. At the same time, the heat signal went down to zero since the catalyst was saturated and therefore unable to adsorb any additional ammonia. This step was followed by a period involving Ar only. An endotherm was observed due to ammonia desorption, which is consistent with ammonia detected by the FTIR. The temperature was then decreased to 400 °C and ammonia was again introduced. Since most of the strongly bound ammonia was already adsorbed at 500 °C, the ammonia adsorbed at 400 °C was somewhat less strongly bound, which accounted for a lowering of the heat to 15.3 mW, thereby producing ΔH of −103 kJ/mol. A corresponding decrease was observed when lowering the temperature to 300 °C

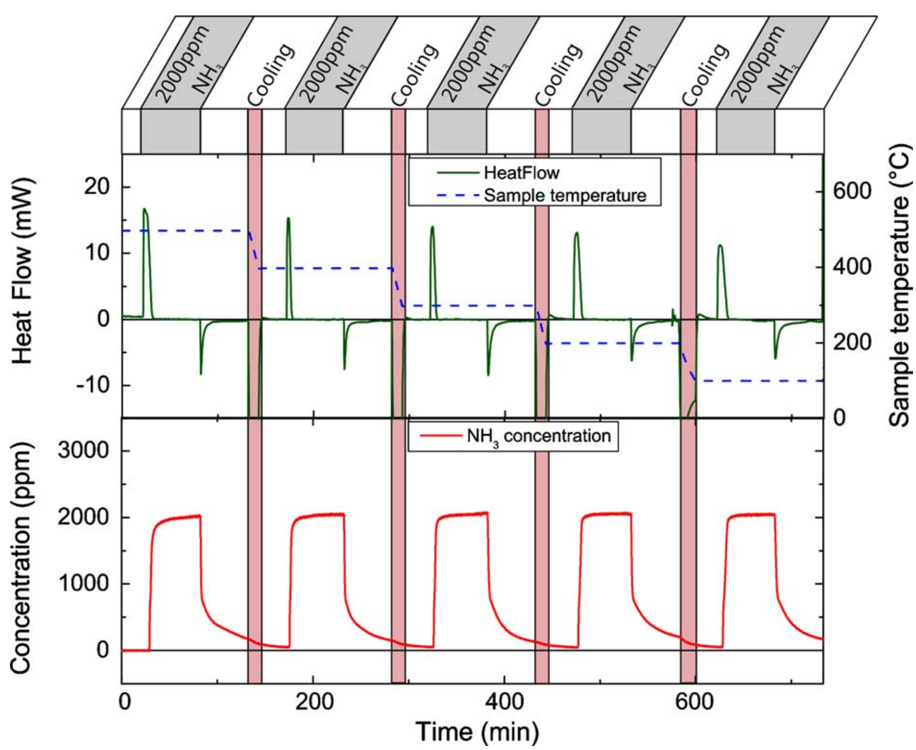

Fig. 4. Thermogram and FTIR signal for an NH_3 stepwise experiment on a Cu-Beta catalyst.

(−94 kJ/mol), 200 °C (−88 kJ/mol) and, finally, to 100 °C (−75 kJ/mol).

When introducing ammonia, an exotherm was observed due to adsorption and when the peak at 500 °C was integrated, the result was 6.4 J. An endotherm was observed when the ammonia was turned off and the catalyst was exposed to Ar alone, due to the desorption of loosely bound ammonia. The corresponding integration of this peak resulted in −1.4 J. The ratio between the heat formed due to adsorption and the heat consumed during desorption was 4.6. Consequently, only a small part of the adsorbed ammonia was desorbed when the ammonia was turned off. When calculating the coverage on the surface, the adsorption alone was included and the small amount of desorbed ammonia was neglected. The reason for the small desorption in this experiment is that the temperature is decreased stepwise and never increased. The sum of adsorbed ammonia at 500, 400, 300 and 200 °C resulted in 191 μmol ammonia, which was similar with the total ammonia adsorption of 190 μmol for the ammonia TPD conducted at 150 °C (see Fig. 4). Calculating the coverage on the surface is difficult since the total amount of ammonia adsorbed depends on the temperature level at which the adsorption was conducted. For example, a large adsorption of physisorbed ammonia was observed at room temperature on Cu-ZSM-5 [32]. In order to estimate the coverage, we use the total adsorption observed at the lowest experimental temperature used (100 °C). Since this low temperature was only used in the ammonia stepwise experiment, where ammonia was adsorbed at several temperatures, we used the sum of adsorbed ammonia at 500, 400, 300, 200 and 100 °C. This resulted in 254 μmol of adsorption sites for ammonia. With the use of this number, we could calculate the coverage at each adsorption temperature and its corresponding heat of adsorption (see Fig. 4). The results are presented in Fig. 5 in which the heat of adsorption of ammonia ($-\Delta H_{ads}$) versus coverage is shown. The results show a linear dependence of the heat of adsorption on the coverage. A corresponding linear fit is also shown in Fig. 5. The heat of adsorption is equal to the activation energy for adsorption minus the activation energy for desorption according to the following:

$$\Delta H = E_{adsorption} - E_{desorption} \tag{7}$$

In general, adsorption often occurs also at very low temperatures, which means that the activation barrier for adsorption is often very small. In many kinetic models the activation barrier for adsorption is assumed to be zero, which is also the case for ammonia adsorption [29,32]. If assuming that the activation barrier for ammonia adsorption is non-activated (0 kJ/mol), the activation energy for ammonia desorption can be described in the following way:

$$E_{desorption} = E_{adsorption} - \Delta H \approx -\Delta H \tag{8}$$

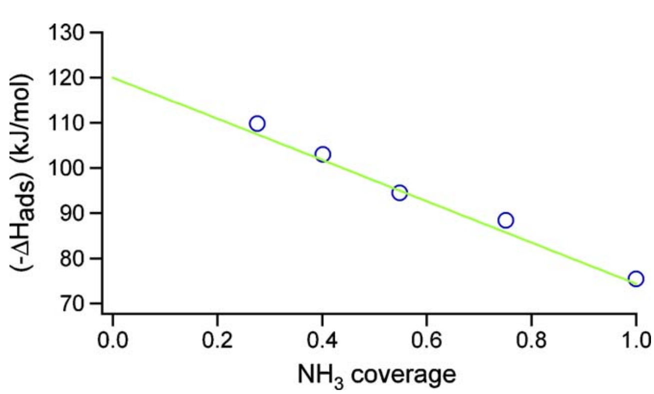

Fig. 5. Heat of adsorption ($-\Delta H$) of ammonia versus ammonia coverage. The circles show the measured values. In addition, a corresponding linear fit is shown.

The equation for the linear fit resulted in

$$-\Delta H = 120.0(1 - 0.38\theta_{NH_3}) \tag{9}$$

where θ_{NH_3} is the coverage of ammonia. Combining Eqs. (8) and (9) resulted in

$$E_{desorption,NH_3} = 120.0(1 - 0.38\theta_{NH_3}) \tag{10}$$

Busco et al. [42] investigated the heat of adsorption at 303 K, which resulted in about −130 kJ/mol at zero coverage for both H-Beta (SiO_2/Al_2O_3 ratio of 19.6) and H-ZSM-5 (SiO_2/Al_2O_3 ratio of 30). Similar results were obtained by Felix et al. [41], who received ΔH for zero coverage of about −120 to 130 kJ/mol for H-ZSM-5 (SiO_2/Al_2O_3 ratio of 110). We obtained a heat of adsorption for zero coverage of −120.0 kJ/mol, which is similar to the results obtained for acid zeolites.

NO_2 adsorbs strongly on copper zeolites [30] and we have observed large formation of nitrates on the Cu-ZSM-5 surface [15]. Accordingly, we investigated the heat of adsorption of NO_2 using microcalorimetry on our Cu-Beta catalyst, the results of which are shown in Fig. 6. The catalyst was first pretreated with oxygen at 500 °C to ensure that no residual ammonia was left on the surface from earlier experiments. This was followed by lowering the temperature to 150 °C and introducing 2000 ppm NO_2 for 60 min. Initially, when introducing NO_2, a narrow negative peak is observed in the thermogram because of fluctuations of pressure when changing the values in the MFC. The NO_2 concentration in the gas bottle was only 5000 ppm, which caused a decrease of the flow from the Ar MFC with 40%, when changing the concentration to 2000 ppm NO_2 (since a large part of the Ar now also comes from the NO_2/Ar MFC). After this peak, an exotherm was revealed and at the same time, NO_2 was stored and NO formed. It is observed for several systems that NO_x stores through disproportionation mechanism, where NO_2 reacts to form nitrates and produces NO in the gas phase. This phenomenon was observed on Cu-ZSM-5 [30,48] and Fe zeolite [20] and also on BaO/Al_2O_3 [49], Al_2O_3 [50], BaNa-Y [51] and BaO/TiO_2 [52]. For this reason, we suggest that also nitrates are stored on Cu-Beta according to the disproportionation mechanism as follows:

$$3NO_2 + Cu{-}O \leftrightarrow Cu(NO_3)_2 + NO(g) \tag{11}$$

This reaction is also in accordance with studies by Despres et al. [48], who observed that NO destabilized the nitrates. This is also shown by the reversible reaction in Eq. (11). Further, Olsson et al. [30] found this reaction to be significant in their detailed kinetic model for NO oxidation on Cu-ZSM- used in a detailed model for ammonia SCR [31]. The integration of the results in Fig. 6 gives 59 μmol NO_2 consumed, while producing 21 μmol NO. This result in a ratio of 2.9 for the NO_2 consumed over the NO produced. Thus, the stoichiometry (3:1) is in line with the proposed disproportionation mechanism shown in Eq. (11). Further, the amount of nitrates formed is about one fifth of the amount of adsorbed ammonia (38 μmol versus 190 μmol). This result is in line with the detailed kinetic models presented by Olsson et al. [30] and Sjövall et al. [32], where a much greater amount of ammonia was adsorbed compared to nitrates on the copper sites.

There was an exotherm associated with the NO_2 adsorption, resulting in a maximum heat release of 9.7 mW. This corresponded to a heat of adsorption of −65 kJ/mol per NO_2 (−196 kJ/mol per $Cu(NO_3)_2$) according to the stoichiometry presented in Eq. (11). It should be pointed out that the heat of adsorption for this reaction is defined as the activation barrier for the forward reaction minus the backward reaction according to the equation below:

$$\Delta H = E_{nitrate\ formation} - E_{nitrate\ decomposition} \tag{12}$$

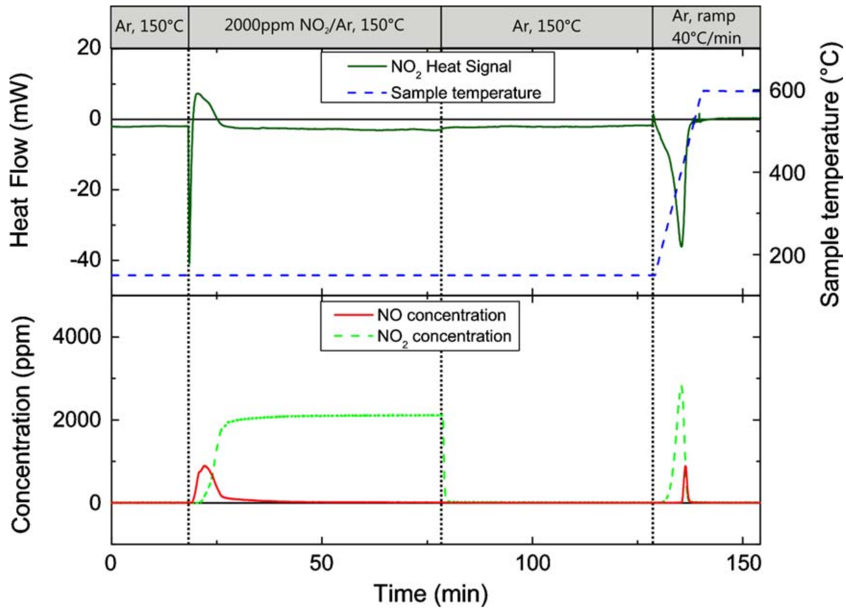

Fig. 6. Thermogram and FTIR signal for an NO_2 TPD experiment on a Cu-Beta catalyst.

During the temperature ramp, a large release of NO_2 was observed due to the decomposition of stored nitrates according to the following reaction:

$$Cu(NO_3)_2 \leftrightarrow 2NO_2 + (1/2)O_2(g) + Cu{-}O \tag{13}$$

At the same time, an endotherm was observed due to the decomposition of the nitrates. In addition, small amounts of NO were observed in the release peak. Since the NO was only visible at the top temperatures, it was probably caused by NO_2 releasing and dissociating to form NO and oxygen [30]. The maximum amount of NO_2 released during the temperature ramp was 2830 ppm and its corresponding endotherm was 34.2 mW. This results in −163 kJ/mol per NO_2 (−325 kJ/mol per $Cu(NO_3)_2$ in Eq. (13)). This means that decomposition without the presence of any NO has much larger activation barrier, something that was also observed in the detailed kinetic model for Cu-ZSM-5 [30].

A corresponding NO TPD was conducted at 150 °C, with the results shown in Fig. 7. A small storage of about 23 μmol NO was observed, which is much smaller than the 38 μmol for NO_2 and 190 μmol for ammonia. The maximum heat observed during the NO adsorption was 4.8 mW and a concurrent breakthrough of 1000 ppm NO was observed, corresponding to −65 kJ/mol per NO adsorbed. After being exposed to NO, the catalyst was flushed with Ar alone and a small desorption of loosely bound NO was observed in the gas phase. Simultaneously, a small endotherm was observed due to the desorption process. Finally, the catalyst was heated at a rate of 40 °C/min and an endotherm was observed because of the desorption of stored NO. However, similar amounts of NO and NO_2 were detected during the desorption peak. Prior to this experiment, the catalyst was pretreated with 8% O_2 at 500 °C and oxygen was likely still present on the copper sites [30] as NO was starting to be introduced during the adsorption phase. For this reason, some of the stored NO probably form NO_2 or alternative nitrates on the

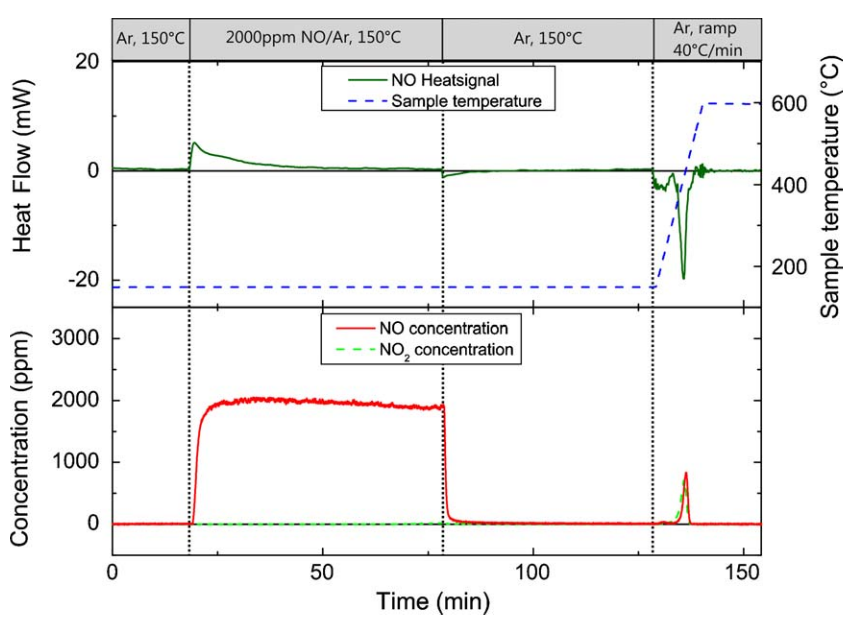

Fig. 7. Thermogram and FTIR signal for an NO TPD experiment on a Cu-Beta catalyst.

catalyst. Thus, the stored NO was likely only about 11 μmol instead of 23 μmol, which is much less than the amount of stored NO_2 in the NO_2 TPD experiment (38 μmol). Also the ΔH was -65 kJ/mol both for the NO and NO_2 adsorption, probably reflecting the fact that substantial amounts of NO_2/nitrates were also generated when exposing the catalyst to NO, due to the preadsorbed oxygen.

4. Conclusions

When developing kinetic models, adsorption heats are key parameters. Microcalorimetry is a powerful tool with which to measure the heat of adsorption independently. Further, in order to describe transient experiments of NH_3 SCR, it is important to first obtain an accurate description of the storage behavior of the catalyst. The objective of this study is to measure the heat of adsorption of NH_3, NO_2 and NO over Cu-Beta.

We prepared a Cu-Beta powder, with a silica to alumina ration of 38. Further the powder was impregnated on a monolith, which had a good NH_3 SCR activity, showing the relevance of studying this catalyst.

Ammonia TPD experiments were conducted at 150 °C using the microcalorimeter; an exotherm was observed when introducing ammonia, due to ammonia adsorption. This resulted in an average heat of adsorption of -100 and -97 kJ/mol, respectively, for two repeated experiments. Thus a good reproducibility was found. During the temperature increase an ammonia release was observed concurrently with an endothermic peak. The ammonia desorption occurred over a broad temperature interval, which can be described using a coverage dependent activation energy. In order to investigate this further, we have designed an ammonia stepwise experiment. The catalyst was initially exposed to 2000 ppm NH_3 at 500 °C with the consequence that ammonia adsorbed at such high temperature was only strongly bound. Thereafter, the catalyst was cooled to 400 °C, while simultaneously flushing it with Ar. Ammonia is again introduced and since all the sites with high adsorption energy were already occupied, the sites featuring lower energy were now occupied. These steps were repeated at 300, 200 and 100 °C. Assuming an activation barrier of zero for adsorption, the coverage dependent activation energy for ammonia desorption was found to be as follows:

$$E_{desorption,NH_3} = 120.0(1 - 0.38\theta_{NH_3})$$

The NO_2 adsorption and desorption was investigated using an NO_2 TPD experiment. Approximately three NO_2 were stored for each NO produced, corresponding to the disproportionation mechanism for producing nitrates. Simultaneously, an exotherm was observed in the thermogram, resulting in ΔH ($E_{\text{nitrate formation}} - E_{\text{nitrate decomposition}}$) of -196 kJ/mol per $Cu(NO_3)_2$. The NO adsorption was examined with an NO TPD, resulting in a small storage of NO.

Acknowledgements

This work has been performed at the Competence Centre for Catalysis and Cummins Inc. The authors would like to thank Cummins Inc. for the financial support. One author (Louise Olsson) would also like to acknowledge the Swedish Research Council (Contract: 621-2003-4149 and 621-2006-3706) and Swedish foundation for strategic research (F06-0006) for additional support. The financial support for the FTIR from Knut and Alice Wallenberg Foundation, Dnr KAW 2005.0055; and for the calorimeter from the Swedish Research Council (Contract: 621-2003-4149 and 621-2006-3706) are gratefully acknowledged.

References

[1] N. Takahashi, H. Shinjoh, T. Iijima, T. Suzuki, K. Yamazaki, K. Yokota, H. Suzuki, N. Miyoshi, S. Matsumoto, T. Tanizawa, T. Tanaka, S. Tateishi, K. Kasahara, Catal. Today 27 (1996) 63.
[2] W. Bogner, M. Kramer, B. Krutzsch, S. Pischinger, D. Voigtlander, G. Wenninger, F. Wirbeleit, M.S. Brogan, R.J. Brisley, D.E. Webster, Appl. Catal. B: Environ. 7 (1995) 153.
[3] J.P.B.R. Burch, C.J. Hill, B. Krutzsch, B. Konrad, E. Jobson, L. Cider, K. Eranen, F. Klingstedt, L.E. Lindfors, Top. Catal. 30–31 (2004) 19.
[4] P. Sazama, L. Capek, H. Drobna, Z. Sobalik, J. Dedecek, K. Arve, B. Wichterlova, J. Catal. 232 (2005) 302.
[5] J.A. Dumesic, N.-Y. Topsoe, H. Topsoe, Y. Chen, T. Slabiak, J. Catal. 163 (1996) 409.
[6] N.-Y. Topsoe, H. Topsoe, J.A. Dumesic, J. Catal. 151 (1995) 226.
[7] A. Grossale, I. Nova, E. Tronconi, D. Chatterjee, M. Weibel, J. Catal. 256 (2008) 312.
[8] H. Sjövall, L. Olsson, E. Fridell, R.J. Blint, Appl. Catal. B: Environ. 64 (2006) 180.
[9] O. Krocher, M. Elsener, Ind. Eng. Chem. Res. 47 (2008) 8588.
[10] J.H. Baik, S.D. Yim, I.S. Nam, Y.S. Mok, J.H. Lee, B.K. Cho, S.H. Oh, Ind. Eng. Chem. Res. 45 (2006) 5258.
[11] A. Lundstrom, B. Andersson, L. Olsson, Chem. Eng. J. 150 (2009) 544.
[12] P.A. Schaber, J. Colson, S. Higgins, D. Thielen, B. Anspach, J. Brauer, Thermochim. Acta 424 (2004) 131.
[13] M. Koebel, G. Madia, F. Raimondi, A. Wokaun, J. Catal. 209 (2002) 159.
[14] I.E. Wachs, G. Deo, B.M. Weckhuysen, A. Andreini, M.A. Vuurman, M.d. Boer, M.D. Amiridis, J. Catal. 161 (1996) 211.
[15] H. Sjövall, E. Fridell, R.J. Blint, L. Olsson, Top. Catal. 42–43 (2007) 113.
[16] J.-H. Park, H.J. Park, J.H. Baik, I.-S. Nam, C.-H. Shin, J.-H. Lee, B.K. Cho, S.H. Oh, J. Catal. 240 (2006) 47.
[17] S. Kieger, G. Delahay, B. Coq, B. Neveu, J. Catal. 183 (1999) 267.
[18] J.A. Sullivan, J. Cunningham, M.A. Morris, K. Keneavey, Appl. Catal. B: Environ. 7 (1995) 137.
[19] K. Rahkamaa-Tolonen, T. Maunula, M. Lomma, M. Huuhtanen, R.L. Keiski, Catal. Today 100 (2005) 217.
[20] A. Grossale, I. Nova, E. Tronconi, Catal. Today 136 (2008) 18.
[21] O. Krocher, M. Devadas, M. Elsener, A. Wokaun, N. Soger, M. Pfeifer, Y. Demel, L. Mussmann, Appl. Catal. B: Environ. 66 (2006) 208.
[22] S. Brandenberger, O. Krocher, A. Tissler, R. Althoff, Catal. Rev.-Sci. Eng. 50 (2008) 492.
[23] A. Grossale, I. Nova, E. Tronconi, Catal. Lett. 130 (2009) 525.
[24] M. Iwasaki, K. Yamazaki, K. Banno, H. Shinjoh, J. Catal. 260 (2008) 205.
[25] I. Nova, L. Lietti, E. Tronconi, P. Forzatti, Chem. Eng. Sci. 56 (2001) 1229.
[26] B. Roduit, A. Wokaun, A. Baiker, Ind. Eng. Chem. Res. 37 (1998) 4577.
[27] L. Lietti, I. Nova, E. Tronconi, P. Forzatti, Catal. Today 45 (1998).
[28] D. Chatterjee, T. Burkhardt, M. Weibel, E. Tronconi, I. Nova, C. Ciardelli, SAE, 2006-01-0468, 2006.
[29] L. Olsson, H. Sjövall, R.J. Blint, Appl. Catal. B: Environ. 81 (2008) 203.
[30] L. Olsson, H. Sjövall, R.J. Blint, Appl. Catal. B: Environ. 87 (2009) 200.
[31] H. Sjövall, R.J. Blint, L. Olsson, Appl. Catal. B 92 (2009) 138.
[32] H. Sjövall, L. Olsson, R.J. Blint, J. Phys. Chem. C 113 (2009) 1393.
[33] G. Delahay, S. Kieger, N. Tanchoux, P. Trens, B. Coq, Appl. Catal. B: Environ. 52 (2004) 251.
[34] S.A. Stevenson, J.C. Vartuli, C.F. Brooks, J. Catal. 190 (2000) 228.
[35] S. Malmberg, M. Votsmeier, J. Gieshoff, N. Söger, L. Mußmann, A. Schuler, A. Drochner, Top. Catal. 42–43 (2007) 33.
[36] D. Chatterjee, T. Burkhardt, M. Weibel, I. Nova, A. Grossale, E. Tronconi, SAE Paper, 2007-01-1136, 2007.
[37] H. Sjövall, R.J. Blint, A. Gopinath, L. Olsson, Ind. Eng. Chem. Res. 49 (2010) 39.
[38] B.E. Spiewak, J.A. Dumesic, Thermochim. Acta 312 (1998) 95.
[39] N. Cardonamartinez, J.A. Dumesic, Adv. Catal. 38 (1992) 149.
[40] H.L. Fang, H.F.M. DaCosta, Appl. Catal. B-Environ. 46 (2003) 17.
[41] P. Felix, C. Savill-Jowitt, D.R. Brown, Thermochim. Acta 433 (2005) 59.
[42] C. Busco, A. Barbaglia, M. Broyer, V. Bolis, G.M. Foddanu, P. Ugliengo, Thermochim. Acta (December) (2004).
[43] G. Boskovic, T. Vulic, E. Kis, P. Putanov, Chem. Eng. Technol. 24 (2001) 269.
[44] H.S. Fogler, Elem. Chem. React. Eng. (2001).
[45] E. Tronconi, I. Nova, C. Ciardelli, D. Chatterjee, B. Bandl-Konrad, T. Burkhardt, Catal. Today 105 (2005) 529.
[46] D. Chatterjee, T. Burkhardt, M. Weibel, E. Tronconi, I. Nova, C. Ciardelli, SAE, 2006.
[47] D. Chatterjee, T. Burkhardt, M. Weibel, I. Nova, A. Grossale, E. Tronconi, SAE, 2007-01-1136, 2007.
[48] M.K.J. Despres, O. Kröcher, M. Elsener, A. Wokaun, Micropor. Mesopor. Mater. 58 (2003) 175.
[49] L. Olsson, H. Persson, E. Fridell, M. Skoglundh, B. Andersson, J. Phys. Chem. B 105 (2001) 6895.
[50] T.S.N. Apostolescu, S. Kureti, Appl. Catal. B 51 (2004) 43.
[51] Y.H. Yeom, J. Henao, M.J. Li, W.M.H. Sachtler, E. Weitz, J. Catal. 231 (2005) 181.
[52] M.K.J. Despres, O. Kröcher, M. Elsener, A. Wokaun, Appl. Catal. B 43 (2003) 389.